

Discontinuous Phase Transitions of Membranes: a Monte Carlo Study

Annette Ammann and Reinhard Lipowsky (*)

Institut für Festkörperforschung, Forschungszentrum Jülich, 52425 Jülich, Germany
and
Max-Planck-Institut für Kolloid- und Grenzflächenforschung, Kantstrasse 55,
14513 Teltow-Seehof, Germany

(Received 4 October 1995, received in final form 17 October 1995, accepted 25 October 1995)

PACS.82.70.-y – Disperse systems

PACS.64.60.-i – General studies of phase transitions

Abstract. — Fluid membranes which experience interaction potentials with a potential barrier are studied by Monte Carlo simulations. For a symmetric double-well potential, the membranes are found to exhibit the same critical behavior as the 2-dimensional Ising model even for zero lateral tension. For an asymmetric adhesion potential with a relatively large potential barrier, the unbound phase is found to nucleate via the formation of membrane ‘islands’ which implies a discontinuous unbinding transition.

1. Introduction

Lipids and other amphiphilic molecules in water form thin bilayer membranes with a thickness of the order of 4-5 nm [1]. These membranes are rather flexible and undergo thermally-excited fluctuations which are directly visible in the optical microscope. Many preparation methods lead to bunches or stacks in which these membranes adhere to one another. Likewise, single membranes usually form closed vesicles which may adhere to other vesicles or to another surface such as the container wall.

If these membranes are electrically neutral, their direct interaction consists of repulsive hydration and attractive van der Waals forces and the corresponding interaction potential exhibits a single minimum. If the membranes carry electric charges, their direct interaction also depends on the electrostatic forces and may then exhibit an attractive potential well at small separations and a repulsive potential barrier at intermediate separations of the membranes [2–4].

As the temperature is increased, the shape fluctuations act to reduce the strength of the potential barrier. For tensionless membranes, one eventually reaches a characteristic temperature $T = T_u$ at which the membranes unbind from one another. It has been recently argued by scaling arguments that this unbinding (or adhesion) transition is continuous for sufficiently weak barriers but discontinuous for sufficiently strong ones [5]. This implies that interacting membranes cannot ‘tunnel’ through strong barriers but are trapped by these barriers as the

(*) Author for correspondence (e-mail: lipowsky@mpikg-teltow.mpg.de)

unbinding temperature is approached from below. The latter prediction does not agree with the results of functional renormalization [6] which imply that fluid membranes behave as 1-dimensional strings in two dimensions which can ‘tunnel’ through any barrier (provided the barrier is short-ranged as will be assumed here).

In order to check the validity of the scaling arguments, we have performed extensive Monte Carlo simulations as will be described in the following. First, a membrane which is subject to a symmetric double-well potential is considered. In this case, the membrane is found to exhibit the same critical properties as the 2-dimensional Ising model. This implies that the membrane undergoes a discontinuous phase transition as a symmetry-breaking field is varied at low temperature. Secondly, an asymmetric adhesion potential with a potential barrier will be studied. In the latter case, the nucleation and growth of membrane ‘islands’ can be directly observed which implies a discontinuous unbinding transition.

2. Theoretical Description and Boltzmann Weight

The shape of a fluid membrane which has zero shear modulus and is taken to be essentially incompressible is governed by its bending rigidity, κ [7–9]. We will focus on lipid bilayers which usually have a bending rigidity large compared to the thermal energy, T (here and below, temperature T is measured in energy units, i.e., the Boltzmann factor k_B has been absorbed into T). In this case, the persistence length of the membrane [10] is very large and the membrane surface exhibits orientational order on the accessible length scales.

Now, consider such an oriented membrane close to a planar reference surface. The separation of the membrane from this surface is described by the displacement field $l(x_1, x_2)$. The configuration energy (or effective Hamiltonian) of this displacement field is given by [11]

$$\mathcal{H}\{l\} = \int d^2x \left\{ \frac{1}{2} \kappa (\nabla^2 l)^2 + \frac{1}{2} \Sigma (\nabla l)^2 + V(l) \right\} \quad (1)$$

where $\Sigma \geq 0$ represents the lateral tension and $V(l)$ the interaction potential arising, e.g. from other membranes or from external forces. In the following, we will study several potentials $V(l)$ which exhibit a potential barrier.

The statistical weight for a certain configuration is given by the Boltzmann factor $\sim \exp[-\mathcal{H}\{l\}/T]$ and the free energy \mathcal{F} of the system is

$$\mathcal{F} = -T \ln \left[\int \mathcal{D}\{l\} e^{-\mathcal{H}\{l\}/T} \right]. \quad (2)$$

where $\int \mathcal{D}\{l\}$ denotes a path integral over all l -configurations. In the thermodynamic limit of large L , the free energy behaves as

$$\mathcal{F} \approx FL^2. \quad (3)$$

The form of the correction terms depends on the boundary conditions. We will use periodic boundary conditions in the \mathbf{x} -direction; in this case, the correction terms are expected to be exponentially small in L .

3. Symmetric Double Well Potential

First, we will consider a membrane which is placed in the symmetric double-well potential as given by

$$V(l) = Al^2 + Bl^4 + Hl. \quad (4)$$

For $H = 0$ and $A < 0$, this potential is symmetric with respect to $l \rightarrow -l$ and exhibits two degenerate minima. The critical behavior discussed below applies to all other potentials which are symmetric and have two degenerate minima separated by a barrier; another example is provided by the interaction potential felt by a membrane between two adhesive walls. For finite lateral tension $\Sigma > 0$, the large scale properties of the membrane are governed by this tension and the model as given by (1) and (4) is equivalent to the effective Hamiltonian (the so-called ' ϕ^4 -theory') used for a bulk critical point in two dimensions. It is well-known that the latter model belongs to the same universality class as the 2-dimensional Ising model [12, 13].

Thus, the phase diagram of the model as given by (1) and (4) with $\Sigma > 0$ can be deduced from the phase diagram for the 2-dimensional Ising model as was mentioned in reference [14]. There is a critical point for $H = 0$ and $A = A_c < 0$ at which the system undergoes a continuous phase transition. For $A < A_c$ and $H = 0$, the symmetry $l \rightarrow -l$ is spontaneously broken, and the membrane under tension is located in one of the two degenerate minima of $V(l)$. In addition, the system undergoes a discontinuous phase transition for $A < A_c$ when the symmetry breaking field H is varied through $H = 0$.

3.1. ISLAND EXCITATIONS. — What happens for zero lateral tension $\Sigma = 0$? In this case, the membrane is again located in one of the two degenerate minima at zero temperature $T = 0$. At small but finite $T > 0$, it will exhibit thermally-excited islands, compare Figures 7 and 10 below.

The excess free energy of one island arises from the edge of this island which consists of the membrane segments within the potential barrier. For an island of lateral size $L_{||}$, one has the edge energy $\Delta\mathcal{E}_e \sim \sigma_0 L_{||}$ where the line tension σ_0 is proportional to the height of the potential barrier. The edge entropy, on the other hand, is dominated by the different shapes of the edge and thus, can be estimated as $\Delta\mathcal{S}_e \sim \ln(3^{L_{||}/a_{||}}) \sim L_{||}$, if the edge is viewed as a random walk with three possibilities at each step. Thus, for small T , the excess free energy, $\Delta\mathcal{F}_e = \Delta\mathcal{E}_e - T\Delta\mathcal{S}_e$, is positive and the membrane fluctuations experiences an effective barrier [5].

The above stability argument implies that the symmetry is spontaneously broken at small T but will be restored at a critical temperature $T = T_c$ at which the excess free energy $\Delta\mathcal{F}_e$ vanishes and the system undergoes a continuous phase transition. This critical point will be studied below by Monte Carlo simulations. In order to extract the critical behavior, we will first discuss the dependence of this behavior on the finite system size.

3.2. FINITE SIZE SCALING AT CONTINUOUS PHASE TRANSITIONS. — In computer simulations, one has to study finite membrane segments of lateral size L . It is then convenient to define the spatially averaged quantity

$$\hat{l} \equiv \int d^2x l(\mathbf{x})/L^2 \quad (5)$$

since the probability distribution $\mathcal{P}(\hat{l})$ for this quantity can be directly determined in the simulations. The same procedure has been used in order to study the phase transition in bulk systems, see [15, 16].

The expectation values of \hat{l} are directly related to the order parameter and the corresponding susceptibility of the phase transition considered here. The order parameter is given by the mean location ℓ of the membrane. In the thermodynamic limit $L = \infty$, one has

$$\ell \equiv \langle \hat{l} \rangle = \partial F / \partial H |_{H=0} \quad (6)$$

where F is the free energy per unit area as defined in (3). The corresponding susceptibility per unit area is obtained via

$$\tilde{\chi} \approx -L^{-2}T \frac{\partial \langle \hat{l} \rangle}{\partial H} \Big|_{H=0} = L^{-2} \partial^2 F / \partial H^2 \Big|_{H=0} = \langle \hat{l}^2 \rangle - \langle \hat{l} \rangle^2 \quad (7)$$

in the limit of large L . Note that we have included the additional prefactor T in the definition of $\tilde{\chi}$.

In order to obtain a state of the membrane for which the symmetry is spontaneously broken and which is characterized by a nonzero value of $\langle \hat{l} \rangle$, the thermodynamic limit must be taken before one considers the limit of zero ‘field’ H . This is, however, not possible in a computer simulation. Thus, there is always a nonzero probability for the membrane to ‘tunnel’ between the two degenerate states for the symmetric double well potential: the expectation value $\langle \hat{l} \rangle$ is necessarily zero if one averages over time scales which are large compared to the corresponding tunneling time. On the other hand, if one averages over time scales which are small compared to this tunneling time, the expectation value $\langle \hat{l} \rangle$ has a nonzero value which should approach, for large L , the thermodynamic value as given by (6).

As long as the membrane does not tunnel between the two degenerate states, the expectation value $\langle \hat{l} \rangle$ is well estimated by

$$\ell_{MC} \equiv \langle |\hat{l}| \rangle \simeq \int_0^\infty d\hat{l} \mathcal{P}(\hat{l}) \hat{l}. \quad (8)$$

Likewise, for these time scales, the susceptibility $\tilde{\chi}$ can be approximated by

$$\tilde{\chi}_{MC} \equiv \langle \hat{l}^2 \rangle - \langle |\hat{l}| \rangle^2. \quad (9)$$

Close to a critical point, the finite system size L represents a scaling field as has been shown in the context of bulk critical phenomena [17,18]. In the present context, the singular part of the free energy density is expected to have the scaling property

$$F(\Delta T, H, L) = b^{-2} F(b^{y_t} \Delta T, b^{y_h} H, b^{-1} L). \quad (10)$$

with $\Delta T \equiv T - T_c$ where the scaling indices y_t and y_h determine the critical exponents in the thermodynamic limit $L = \infty$. Indeed, in this limit, the correlation length ξ diverges as

$$\xi \sim 1/|T - T_c|^\nu \quad \text{with} \quad \nu = 1/y_t. \quad (11)$$

Likewise, the mean location ℓ which plays the role of the order parameter decays as

$$\ell \sim |T - T_c|^\beta \quad \text{with} \quad \beta = (2 - y_h)/y_t. \quad (12)$$

and the susceptibility diverges as

$$\tilde{\chi} \sim 1/|T - T_c|^\gamma \quad \text{with} \quad \gamma = (2y_h - 2)/y_t. \quad (13)$$

as follows from (6), (7) and (10) with $L = \infty$. The three critical exponents ν , β and γ satisfy the scaling relation $\gamma = 2(\nu - \beta)$ (which is restricted to systems with $d_{||} = 2$ dimensions).

If one uses the definition of $\ell = \langle \hat{l} \rangle$ as given by (6) even for finite L (and ignores the fact that $\langle \hat{l} \rangle = 0$ in this case), the finite size scaling form (10) for the free energy implies a corresponding scaling form for $\langle \hat{l} \rangle$. This scaling form should also hold for $\ell_{MC} = \langle |\hat{l}| \rangle$ since both expectation

values $\langle \hat{l} \rangle$ and $\langle |\hat{l}| \rangle$ can be obtained from the same probability distribution $\mathcal{P}(\hat{l})$, compare (8). Thus, one expects that

$$\ell_{\text{MC}} = \xi^{-\beta/\nu} \Omega_\ell(L/\xi) = L^{-\beta/\nu} \Phi_\ell(L^{1/\nu} \Delta T). \quad (14)$$

It then follows from the definition of $\tilde{\chi}_{\text{MC}}$ as given by (9) that

$$\tilde{\chi}_{\text{MC}} = L^{-2\beta/\nu} \Phi_\chi(L^{1/\nu} \Delta T) = L^{\gamma/\nu-2} \Phi_\chi(L^{1/\nu} \Delta T) \quad (15)$$

where the scaling relation $\gamma = 2(\nu - \beta)$ has been used. In the following, the measured quantities ℓ_{MC} and $\tilde{\chi}_{\text{MC}}$ are again denoted by ℓ and $\tilde{\chi}$ in order to simplify the notation.

3.3. CUMULANTS OF THE SPATIALLY AVERAGED ORDER PARAMETER. — If the lateral size L is large compared to the correlation length ξ , the spatially averaged order parameter \hat{l} as defined in (5) represents a summation over a large number of essentially uncorrelated and thus independent displacement fields $l(\mathbf{x})$. It then follows from the central limit theorem that \hat{l} should be governed by a probability distribution $\mathcal{P}(\hat{l})$ which is essentially Gaussian.

For $T > T_c$, this distribution has a single maximum at $\hat{l} = 0$ and thus can be written as

$$\mathcal{P}(\hat{l}) \simeq \frac{1}{N} \exp[-L^2 \hat{l}^2 / 2\chi] \quad (16)$$

with $N \equiv [2\pi\chi/L^2]^{1/2}$. This functional form implies that $\tilde{\chi} \approx \langle \hat{l}^2 \rangle = \chi/L^2$, compare (7). For $T < T_c$, on the other hand, the symmetry is spontaneously broken with $\langle \hat{l} \rangle = \ell = \pm l_0$ for $L = \infty$, and the distribution $\mathcal{P}(\hat{l})$ can be approximated by the superposition of two Gaussians:

$$\mathcal{P}(\hat{l}) \simeq \frac{1}{2N} (\exp[-L^2(\hat{l} - l_0)^2 / 2\chi] + \exp[-L^2(\hat{l} + l_0)^2 / 2\chi]) \quad (17)$$

Note that $\tilde{\chi} \approx \chi/L^2$ as defined by (7) contains an explicit factor T .

In order to determine the location of the critical point, it will be convenient to study the cumulants

$$C_2 \equiv \langle \hat{l}^2 \rangle / \langle |\hat{l}| \rangle^2 \quad (18)$$

and

$$C_4 \equiv \langle \hat{l}^4 \rangle / \langle \hat{l}^2 \rangle^2 \quad (19)$$

Using the Gaussian distributions as given by (16) and (17), these cumulants can be calculated in closed form.

For $T < T_c$, the superposition of two Gaussian distributions as given by (17) leads to

$$\langle |\hat{l}| \rangle = (2\chi/\pi L^2)^{1/2} \exp[-L^2 l_0^2 / 2\chi] + l_0 \text{erf}[L l_0 / \sqrt{2\chi}], \quad (20)$$

where $\text{erf}[y]$ denotes the error function [19],

$$\langle \hat{l}^2 \rangle = (1 + L^2 l_0^2 / \chi) \chi / L^2, \quad (21)$$

and

$$\langle \hat{l}^4 \rangle = (3 + 6L^2 l_0^2 / \chi + L^4 l_0^4 / \chi^2) \chi^2 / L^4. \quad (22)$$

The corresponding expressions for $T > T_c$ as calculated with the single Gaussian (16) are easily obtained from (20)-(22) by setting $l_0 = 0$.

It now follows that the cumulant C_2 as defined in (18) behaves, in the limit of large L , as

$$\begin{aligned} C_2 &\approx l_0^2/[l_0 \operatorname{erf}(Ll_0/\sqrt{2\chi})]^2 \approx 1 && \text{for } T < T_c \\ &= \pi/2 \simeq 1.57. && \text{for } T > T_c \end{aligned} \quad (23)$$

Likewise, the cumulant C_4 has the asymptotic behavior

$$\begin{aligned} C_4 &\approx 1 && \text{for } T < T_c \\ &= 3 && \text{for } T > T_c \end{aligned} \quad (24)$$

for large L . This different behavior for $T < T_c$ and $T > T_c$ will be used below in order to determine the location of the critical temperature T_c as has been previously done in the context of bulk systems [13, 15, 20].

3.4. MONTE CARLO SIMULATION. — In the Monte Carlo work, the membrane is discretized on a square lattice with lattice sites $i = 1, \dots, (L/a)^2$ and lattice constant a . The discretized Laplace operator is then given by

$$\nabla_d^2 l_i = l_{i,j+1} + l_{i,j-1} + l_{i-1,j} + l_{i+1,j} - 4l_{i,j}. \quad (25)$$

In order to obtain a fully vectorized code, the lattice has been divided into five independent sublattices.

It is convenient to introduce the dimensionless displacement field $z \equiv l/a$ and the dimensionless potential

$$U(z) \equiv a^2 V(az)/T = (a^4 A/T)z^2 + (a^6 B/T)z^4 + (a^3 H/T)z. \quad (26)$$

The Boltzmann weight is now given by $\exp[-\mathcal{H}\{z\}/T]$ with the configuration energy

$$\mathcal{H}\{z\}/T = \sum_i \left[\frac{1}{2} (\kappa/T) (\nabla_d^2 z_i)^2 + U(z_i) \right] \quad (27)$$

The data discussed here have been obtained for the parameter values $\kappa/T = 0.32$, $a^6 B/T = 10$, and $H = 0$ as a function of the reduced temperature variable

$$\tau \equiv a^4 A/T \quad (28)$$

and of the system size L .

In order to get acceptable errors for the measured quantities, between 10^7 and 10^8 Monte-Carlo steps per lattice site were necessary. The sublattice sizes n_s which have been studied were $n_s = 3, 4, 6, 8, 10, 14$ and 20 , which correspond to the total number of lattice sites $(L/a)^2 = 5n_s^2 = 45, 80, 180, 320, 500, 980$, and 2000 . In all Monte Carlo runs, the mean location ℓ , the susceptibility $\tilde{\chi}$ and the two cumulants C_2 and C_4 as defined in (18) and (19) have been measured.

These two cumulants provide a rather convenient method by which one can determine the locus of the critical point. Indeed, each cumulant approaches two different constants for small and for large T as given by (23) and (24). These values apply to the limit in which the system size L is large compared to the correlation length ξ . Close to the critical temperature $T = T_c$, this limit cannot be observed in the simulations and one measures intermediate values for C_2 and C_4 . The corresponding data are displayed in Figures 1 and 2.

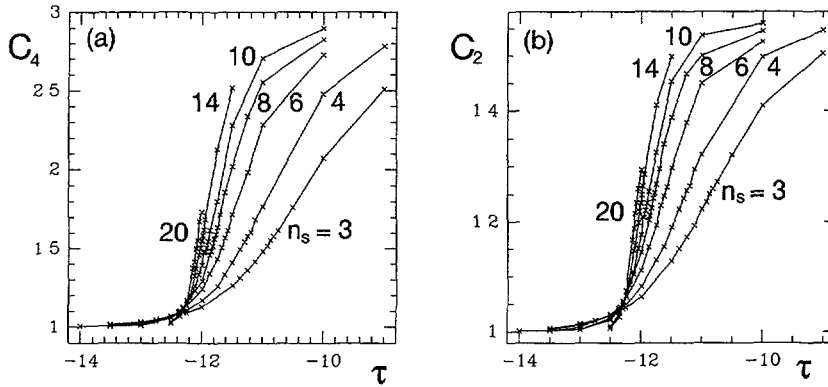


Fig. 1. — The 4th and the 2nd cumulant C_4 and C_2 of the spatially averaged order parameter as a function of the reduced temperature τ for different values of the linear system size $L/a = \sqrt{5}n_s$.

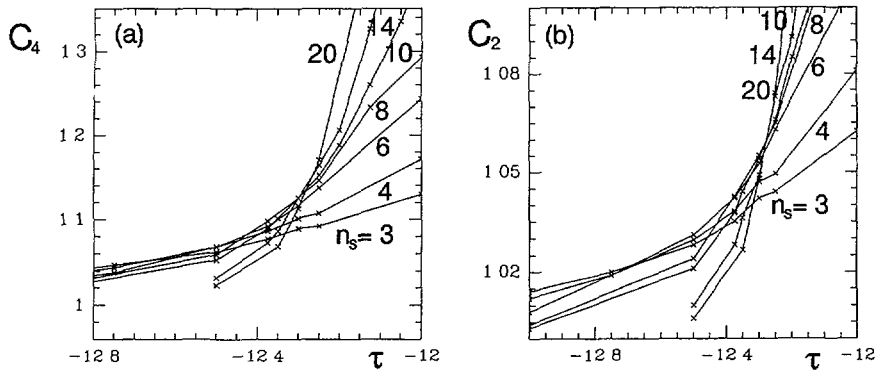


Fig. 2. — The 4th and the 2nd cumulant C_4 and C_2 in the vicinity of the phase transition: The intersection points of the curves for large lattice sizes lead to the estimate $\tau_c = -12.275 \pm 0.025$ for the critical temperature.

In these figures, the cumulants C_2 and C_4 are plotted as a function of the reduced temperature variable τ for different values of the sublattice size n_s . Inspection of these figures shows that the data are consistent with the analytic expressions in (23) and (24): (i) The fourth order cumulant C_4 approaches the constant value $C_4 \approx 1$ for large negative τ or small T and is smaller than the large T value $C_4 = 3$ for small τ ; and (ii) The second order cumulant C_2 approaches the constant value $C_2 \approx 1$ for large negative τ or small T and is smaller than the large T value $C_2 = \pi/2 \approx 1.57$ for small τ .

At intermediate temperatures, the curves corresponding to different system sizes intersect. The location of these intersection points provides an estimate for the critical temperature $T = T_c$. Extrapolation to large n_s or $L/a = \sqrt{5}n_s$ gives the estimate $\tau_c = -12.275 \pm 0.025$ for the critical value of the reduced temperature variable τ .

In Figure 3, the mean location ℓ and the susceptibility per unit area $\bar{\chi}$ are plotted as a function of τ for different values of the sublattice size n_s . These data are now analyzed using the finite size scaling forms for ℓ and $\bar{\chi}$ as given by (14) and (15).

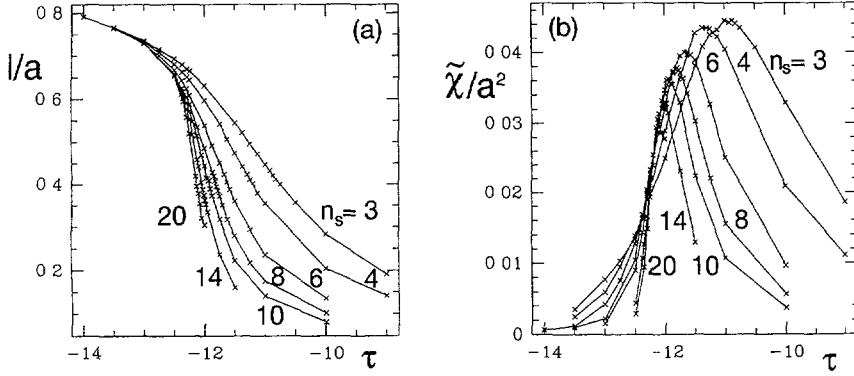


Fig. 3. — (a) Mean location l/a and (b) Susceptibility per unit area $\tilde{\chi}/a^2$ as a function of the reduced temperature τ for different values of the linear system size $L/a = \sqrt{5}n_s$.

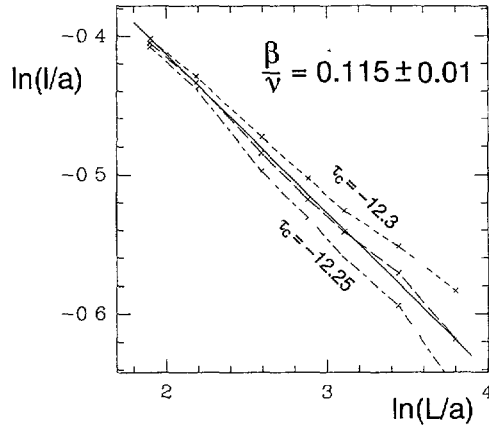


Fig. 4. — Double-logarithmic plot of the mean location l/a as a function of the linear system size L/a . The value $\tau_c = -12.275$ for the critical temperature leads to the estimate $\beta/\nu = 0.115 \pm 0.01$ for the ratio of the critical exponents β and ν .

It follows from (14) that the mean location l should scale at $\Delta T = 0$ or $\tau = \tau_c$ as $l \sim L^{-\beta/\nu}$ with the finite system size L . This behavior is shown in Figure 4 in which l at $\tau = \tau_c$ is plotted double-logarithmically as a function of the system size L for three different values of τ_c . Using the best estimate $\tau_c \simeq -12.275$, the slope of the interpolating curve gives the estimate $\beta/\nu = 0.115 \pm 0.01$.

The data for the susceptibility per unit area, $\tilde{\chi}$, as shown in Figure 3b, exhibit a maximum at a certain temperature τ_{\max} or ΔT_{\max} . If one uses the finite size scaling form (15) for $\tilde{\chi}$, one finds from $\partial\tilde{\chi}/\partial\Delta T = 0$ at $\Delta T = \Delta T_{\max}$ that $L^{1/\nu}\Delta T_{\max} = \text{const}$. This implies the scaling behavior $\Delta T_{\max} \sim (\tau_{\max} - \tau_c) \sim L^{-1/\nu}$ and, thus, $\tilde{\chi}_{\max} \sim L^{\gamma/\nu-2}$. The two quantities $\tilde{\chi}_{\max}$ and $\Delta\tau_{\max} \equiv \tau_{\max} - \tau_c$ are plotted in Figures 5a and 5b, respectively, where the estimate $\tau_c \simeq -12.275$ has been used for the data in Figure 5b. The slope of the two interpolating curves in these double-logarithmic plots gives the estimates $\gamma/\nu \simeq 1.76 \pm 0.02$ and $1/\nu \simeq 1.05 \pm 0.1$,

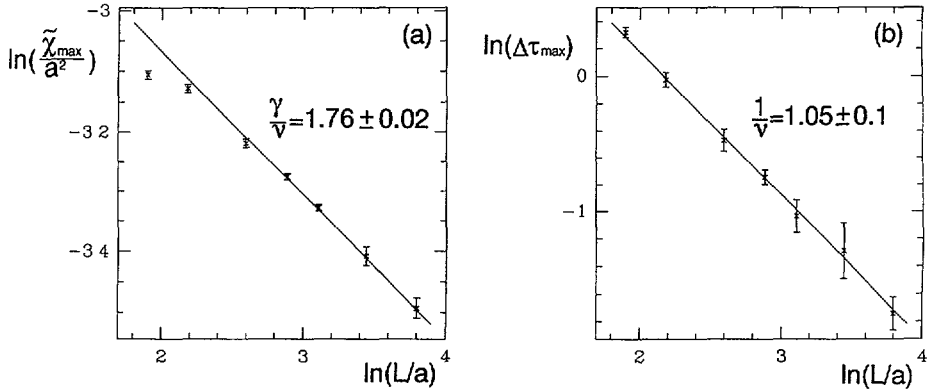


Fig. 5. — (a) The maximum of the susceptibility per unit area $\tilde{\chi}_{\max}/a^2$, and (b) The reduced temperature difference $\Delta\tau_{\max} = (\tau_{\max} - \tau_c)$ are shown in a double-logarithmic plot as a function of the system size L/a . The slope of the interpolation curves leads to the critical exponent ratios $\gamma/\nu = 1.76 \pm 0.02$ and $1/\nu = 1.05 \pm 0.1$.

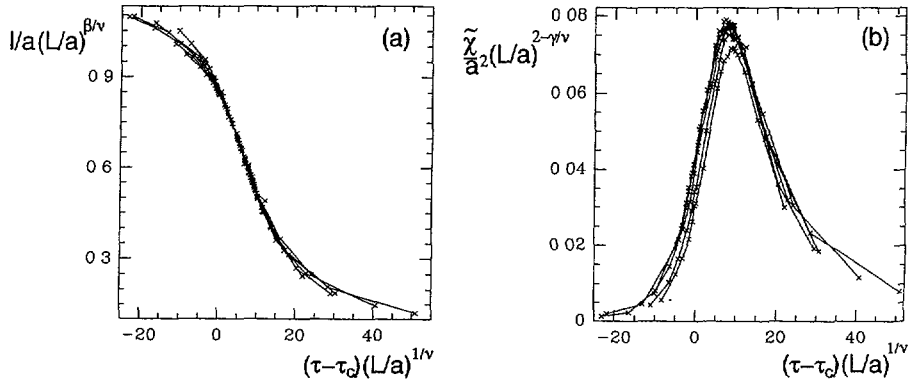


Fig. 6. — (a) The rescaled membrane location $\ell/a(L/a)^{\beta/\nu}$ and (b) The rescaled susceptibility $(\tilde{\chi}/a^2)(L/a)^{2-\gamma/\nu}$ are plotted as a function of the rescaled temperature $(\tau - \tau_c)(L/a)^{1/\nu}$ for different system sizes L/a using the value $\tau_c = -12.275$ for the critical temperature and the values $\gamma = 7/4, \beta = 1/8$ and $\nu = 1$ for the critical exponents.

respectively. In this way, one obtains the numerical estimates

$$\nu = 0.95 \pm 0.1, \quad \gamma = 1.67 \pm 0.2 \quad \text{and} \quad \beta = 0.11 \pm 0.02 \quad (29)$$

for the three critical exponents ν , γ , and β . The scaling relation $\gamma = 2(\nu - \beta)$ is fulfilled within the accuracy of the data.

The consistency of the numerical estimates for the critical temperature and the critical exponents can be checked if one plots the rescaled quantities $\ell L^{\beta/\nu}$ and $\tilde{\chi} L^{2-\gamma/\nu}$ as a function of the rescaled temperature deviation $L^{1/\nu} \Delta T \sim (L/a)^{1/\nu} (\tau - \tau_c)$ as shown in Figure 6. Inspection of these figures shows that the data for different values of L almost collapse onto one curve.

Within the accuracy of the simulations, the values of the critical exponents as found here are identical with the corresponding values for the 2-dimensional Ising model which are given

by $\nu = 1$, $\gamma = 7/4$, and $\beta = 1/8$ [12, 21]. Thus, the critical point studied here for a tensionless membrane in a symmetric double-well potential should belong to the same universality class as the critical point in the 2-dimensional Ising model.

As discussed above, it is rather obvious that the same universality class applies to a membrane under lateral tension (or to an interface). Thus, close to the critical point, the renormalization of the fluctuating field l generates a square-gradient or tension term $\sim (\nabla l)^2$ even if it is originally absent. This is related to the fact that the phase transition occurs in the presence of a confining potential which breaks the rotational symmetry of the bending energy. In contrast, this symmetry is restored at an unbinding transition as considered in the next section since the unbound state does not feel any potential. Thus, the unbinding transition of a tensionless membrane [22] does not belong to the same universality class as the unbinding transition of a membrane under lateral tension (which is similar to a wetting transition).

4. Asymmetric Interaction Potential

The interaction potential $V(l)$ of two membranes at separation l is very asymmetric: it contains a hard wall interaction with $V(l) = \infty$ for $l < 0$, but decays to zero for large l . As mentioned, the interaction potential of charged membranes often exhibits an attractive potential well at small separation and a repulsive potential barrier at intermediate separations of the membranes. Such a potential will be considered in the following section.

The adhesion potential which will be studied by Monte Carlo simulations corresponds to a truncated double well potential, and is given by

$$\begin{aligned} V(l) &= V_{\text{ba}} + A(l - l_{\text{ba}})^2 + B(l - l_{\text{ba}})^4 \quad \text{for } l < l_* \\ &= 0 \quad \text{for } l > l_* \end{aligned} \quad (30)$$

with $A < 0$, $0 < V_{\text{ba}} < |A|^2/4B$ and

$$l_* \equiv l_{\text{ba}} + \sqrt{|A|/2B} [1 - \sqrt{1 - 4BV_{\text{ba}}/A^2}]^{1/2} \quad (31)$$

The barrier is located at $l = l_{\text{ba}}$ with $V(l_{\text{ba}}) = V_{\text{ba}}$. In terms of the dimensionless displacement field $z = l/a$, one has the dimensionless potential

$$\begin{aligned} U(z) &= U_{\text{ba}} + \tau(z - z_{\text{ba}})^2 + b(z - z_{\text{ba}})^4 \quad \text{for } z < z_* \\ &= 0 \quad \text{for } z > z_* \end{aligned} \quad (32)$$

with $\tau < 0$. The asymmetric interaction potential as given by (30) exhibits a narrow potential well for $l = l_{\text{min}} < l_{\text{ba}}$ and an 'infinitely broad' well for $l > l_{\text{ba}}$.

4.1. ISLAND EXCITATIONS AND UNBINDING TRANSITION. — Now, consider a membrane which is bound to the adhesion potential, i.e., which is located within the potential well at small l , and which exhibits an island excitation of lateral size L_{\parallel} . The membrane segment of the island is located outside of the potential barrier. The excess free energy of this island is given by

$$\Delta\mathcal{F} \approx \Delta F L_{\parallel}^2 + \sigma L_{\parallel}. \quad (33)$$

The first term $\sim L_{\parallel}^2$ depends on the difference ΔF between the free energy of the bound and the unbound state: for the bound and unbound state, one has $\Delta F > 0$ and $\Delta F < 0$, respectively.

The unbinding transition occurs at $\Delta F = 0$. The second term $\sim L_{||}$ represents the (large scale) edge energy of the island where the line tension σ is positive as long as the membrane feels an effective potential barrier. As discussed in reference [5], the unbinding transition is continuous if $\sigma \leq 0$ but discontinuous if $\sigma > 0$ at the transition determined by $\Delta F = 0$. Thus, a sufficiently large potential barrier V_{ba} which implies a positive line tension σ will lead to a discontinuous unbinding transition.

For the interaction potential as given by (30), the free energy difference ΔF can be estimated as follows. In the unbound state, the interaction potential vanishes and the entropy loss per unit area of the $L_{||}$ -segment is of order $T/L_{||}^2$ [23, 24]. In the bound state, the interaction potential is

$$V_{we} \equiv V(l_{\min}) = V_{ba} - |A|^2/4B \quad (34)$$

and the free energy contained in the harmonic fluctuations is $\sim T\sqrt{|A|/\kappa}$. The latter estimate follows from the usual relation [10, 22] $\xi_{||} \sim (\kappa/v_2)^{1/4}$ with $v_2 \equiv (\partial^2 V/\partial l^2)$ at $l = l_{\min}$ for the longitudinal correlation length $\xi_{||}$. This leads to

$$\Delta F \simeq V_{we} + cT\sqrt{|A|/\kappa}. \quad (35)$$

At the unbinding transition, one has $\Delta F = 0$ which implies $V_{we} < 0$ as one expects intuitively.

4.2. DECAY OF METASTABLE STATES VIA THE NUCLEATION OF ISLANDS. — Now, consider the case of a discontinuous unbinding transition at the transition temperature $T = T_u$ for which the (large-scale) line tension $\sigma > 0$, and assume that the transition is approached from the bound state with $\Delta F > 0$. This bound state becomes metastable beyond the transition point where $\Delta F < 0$. It then decays via the nucleation of islands which consist of membrane segments located on the other side of the potential barrier. In this case, one has the island free energy

$$\Delta \mathcal{F} \approx -|\Delta F|L_{||}^2 + \sigma L_{||} \approx -|f_1|(T - T_u)L_{||}^2 + \sigma L_{||} \quad (36)$$

where the free energy density ΔF has been expanded up to first power in $(T - T_u)$. One may now use classical nucleation theory [25–27] and determine the properties of the critical nuclei or islands from the maximum of $\Delta \mathcal{F}$ as a function of $L_{||}$. In this way, one obtains the size $L_{||}^* = \sigma/2|f_1|(T - T_u)$ and the free energy $\Delta \mathcal{F}^* = \sigma^2/4|f_1|(T - T_u)$ of these critical islands. The probability to excite one such island by thermal fluctuations for a system with L^2 degrees of freedom is proportional to $(L/L_{||}^*)^2 \exp[-\Delta \mathcal{F}^*/T]$.

Therefore, the nucleation time t_{nu} for a single critical island should scale as

$$t_{nu} \sim (L_{||}^*/L)^2 e^{\Delta \mathcal{F}^*/T} = (L_{||}^*/L)^2 e^{T_{sc}/(T-T_u)} \quad (37)$$

with the temperature scale $T_{sc} \equiv \sigma^2/4|f_1|T$. After one critical island has been nucleated, it will grow and will start to pull the whole membrane segment over the barrier. Obviously, the corresponding spreading time t_{sp} will increase with the size L of the membrane segment. The decay of the metastable state will be governed by the nucleation of a single island as long as $t_{nu} \gg t_{sp}$. In the latter case, one has

$$t_d \simeq t_{nu} \sim L^{-2} e^{T_{sc}/(T-T_u)}, \quad (38)$$

and the decay time of the metastable state should scale as $t_d \sim L^{-2}$ and as $\ln(t_d) \sim 1/(T - T_u)$ close to the discontinuous unbinding transition.

As the size L of the membrane segment increases, the nucleation time $t_{\text{nu}}(L)$ decreases and the spreading time $t_{\text{sp}}(L)$ increases. Thus, one may define a crossover size $L = L_*$ for which $t_{\text{nu}}(L_*) \simeq t_{\text{sp}}(L_*)$. If L exceeds L_* , the decay of the metastable state will involve the nucleation of several critical islands. For large $L \gg L_*$, the number density of these critical island should be of the order of $1/L_*^2$ and the decay time t_d should behave as

$$t_d \simeq t_{\text{nu}}(L_*) \sim L_*^{-2} e^{T_c/(T-T_u)} \quad (39)$$

and, thus, should become independent of the system size L .

The decay of metastable states via the nucleation of many critical islands has been previously studied in the context of Ising models [28,29]. It has been found in these studies that the radius of a supracritical island in two dimensions (or a supracritical droplet in three dimensions) increases linearly with time. If one assumes that this growth law is also applicable to the situation studied here, one obtains the spreading time $t_{\text{sp}}(L) \sim L$ which implies the crossover relation $L_*^{-2} \exp[T_{\text{sc}}/(T - T_u)] \sim L_*$ and, thus, the decay time $t_d \sim L \sim \exp[T_{\text{sc}}/3(T - T_u)]$.

4.3. MONTE CARLO SIMULATION. — Now, the nucleation of islands through an intermediate potential barrier will be studied by Monte Carlo simulations for the interaction potential $U(z)$ as given by (32). For all simulations discussed in the following, the potential parameter $b = 1$ and the reduced bending rigidity $\kappa/T = 0.32$ were chosen. For the latter choice of parameters, the symmetric double-well potential has its critical point at $\tau = \tau_c = -2.335 \pm 0.01$ (as determined by additional simulations not discussed here).

If the membrane is initially located within the potential well of the asymmetric adhesion potential, it experiences a potential barrier of height $\Delta U = U_{\text{ba}} - U_{\text{we}} = \tau^2/4b$. We know from the simulations for the symmetric double well that the membrane cannot tunnel through such a potential barrier provided $\tau^2/4b > \tau_c^2/4b$. In addition, the estimate (35) for the excess free energy ΔF implies that $U_{\text{we}} \sim V_{\text{we}}$ is negative at the transition temperature $T = T_u$ and that $\Delta U(T = T_u) = U_{\text{ba}} - U_{\text{we}} > U_{\text{ba}}$. Therefore, the parameter choice $U_{\text{ba}} > \tau_c^2/4b$ leads to $\Delta U(T = T_u) > \tau_c^2/4b$ and, thus, ensures that the membrane is trapped at the transition point.

The Monte Carlo data discussed here have been obtained for the choice $U_{\text{ba}} = 2.6^2/4b = 1.69$ which satisfies $U_{\text{ba}} > \tau_c^2/4b$ for $b = 1$ since $\tau_c \simeq -2.3$ in this case as mentioned. If one now varies the reduced temperature variable τ , the membrane should undergo a discontinuous unbinding transition at $\tau = \tau_u < \tau_c$. The data discussed below lead to the estimate $\tau_u \simeq -3.2$.

If the transition is discontinuous, the bound state still exists as a metastable state for $\tau \gtrsim \tau_u$. One may then observe the nucleation of islands towards the unbound state which represents the stable phase for $\tau > \tau_u$. On the other hand, the parametrization of the interaction potential as given by (32) is only valid for $U_{\text{ba}} < \tau^2/4b$: for $U_{\text{ba}} = \tau^2/4b$ the potential well at small z has the value $U(z_{\text{min}}) = 0$ and z_* has the limiting value $z_* = z_{\text{ba}} + \sqrt{|\tau|/2b}$. For the choice $b = 1$ and $U_{\text{ba}} = 2.6^2/4$, this constraint is equivalent to $\tau < -\sqrt{4bU_{\text{ba}}} = -2.6$. Therefore, the nucleation of islands has been studied for τ -values which lie in the interval $\tau_u \simeq -3.2 < \tau < -\sqrt{4bU_{\text{ba}}} = -2.6$. Note that these τ -values also satisfy $\tau < \tau_c \simeq -2.33$ where τ_c is the value of the critical temperature for the corresponding double-well potential. Therefore, the membrane should experience an effective potential barrier for all of these τ -values.

In the Monte Carlo simulations, the membrane was initially placed in the potential well with constant displacement field $z = z_{\text{min}}$. The membrane then adapts to this potential well and acquires some roughness. For the chosen parameters, this relaxation process is relatively fast, and the corresponding relaxation time t_r is of the order of 10^2 Monte Carlo steps per lattice site. The decay time t_d of this metastable state is identified with the time after which the spatially averaged order parameter $\hat{z} = \sum_i z_i/N$ satisfies $\hat{z} > z_{\text{ba}}$ which implies that the membrane has moved through the barrier. For the parameter values considered here, this time

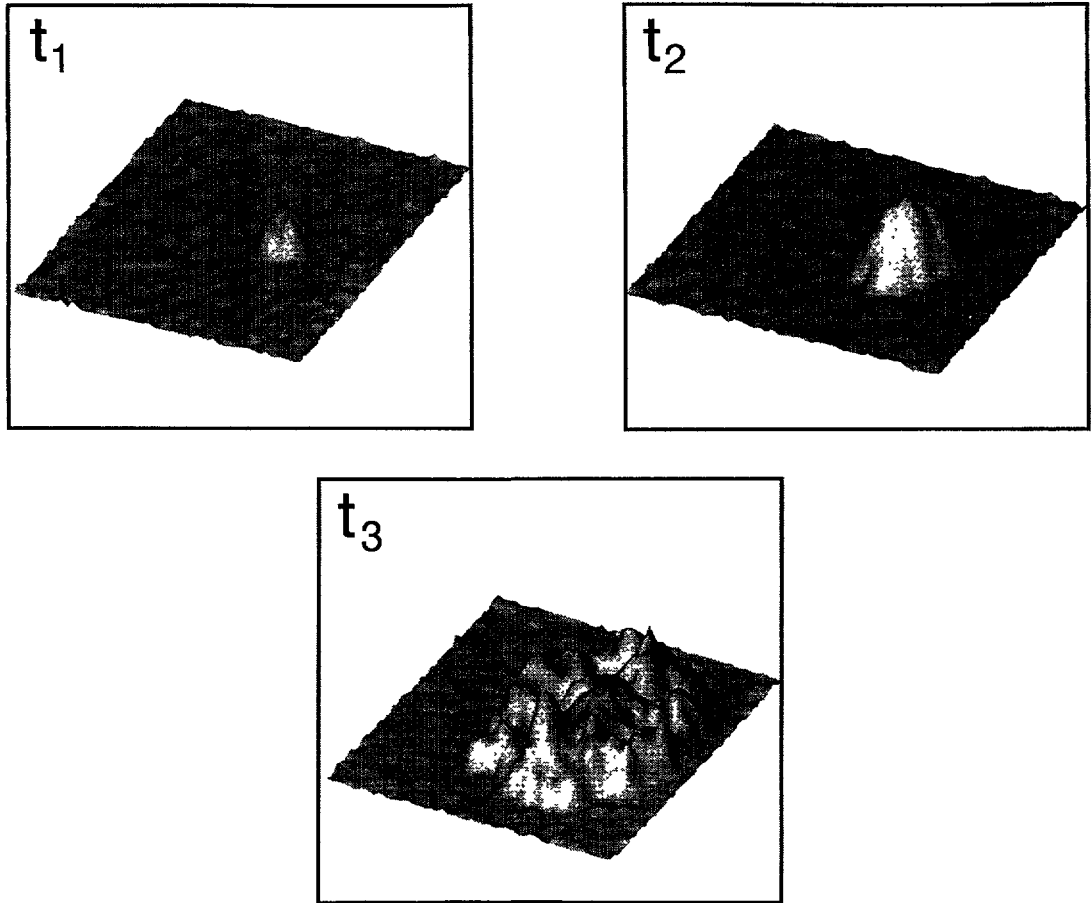


Fig. 7. — Example for the growth of a membrane island through the barrier of an asymmetric interaction potential: snapshots are taken after $t_1 = 2.75 \times 10^4$, $t_2 = 3.25 \times 10^4$ and $t_3 = 4 \times 10^4$ MC-steps for temperature $\tau = -2.95$ and the linear sublattice size $n_s = 50$.

t_d is of the order of $10^3 - 10^8$ Monte Carlo steps per lattice site and, thus, is much larger than the relaxation time t_r . In practice, t_d was obtained from an average over 20 Monte Carlo runs. In order to extend the range of L -values, sublattices with a linear dimension $n_s = 3, 4, 6, 10, 30$, and 50 have been studied which correspond to the total number of lattice sites $N = (L/a)^2 = 45, 80, 180, 500, 4500$, and 12500.

An example for the nucleation of an island is displayed in Figure 7. First, a small hump extends across the barrier which subsequently spreads both in the lateral and in the perpendicular direction. In Figure 8, the quantity $1/\ln(t_d)$ where t_d represents the measured decay time is plotted as a function of the reduced temperature variable τ for several values of the sublattice size n_s . According to the relation (37), this quantity should vanish as $(T - T_u) \sim (\tau - \tau_u)$. Extrapolating the data displayed in Figure 8 towards the τ -axis, one obtains the estimate $\tau_u = -3.23 \pm 0.02$. The data obtained for lattice sizes $N = 45$ and $N = 80$ (i.e. $n_s = 3$ and $n_s = 4$) have not been displayed in Figure 8 since, in these cases, the size $L_{||}^*$ of the critical nucleus is comparable to or exceeds the size L of the whole membrane segment, and the estimate for the decay time as given by (37) does not apply, see below.

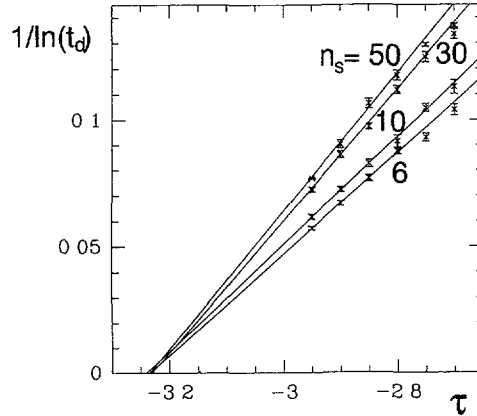


Fig. 8. — Decay time t_d of the metastable state as a function of the reduced temperature τ for different values of the linear sublattice size n_s . Note that larger values of τ correspond to smaller values of t_d and thus to a faster decay. Extrapolation to $1/\ln(t_d) = 0$ gives the estimate $\tau_u = -3.23 \pm 0.02$ for the unbinding temperature.

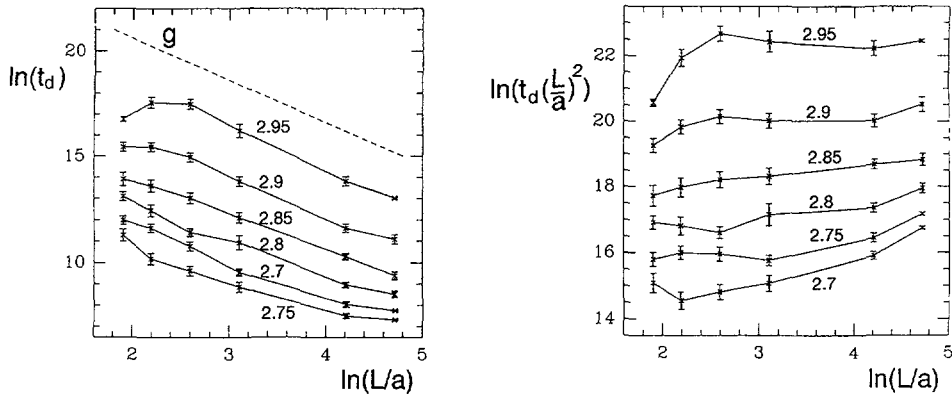


Fig. 9. — Double-logarithmic plots of (a) the decay time t_d and (b) the rescaled decay time $t_d(L/a)^2$ as a function of the linear dimension L/a for different values of the negative reduced temperature $-\tau$. For comparison, the dashed straight line denoted by g which corresponds to $t_d \sim 1/L^2$ has also been included.

In Figure 9, the measured decay time t_d is shown as a function of the system size L/a for several values of τ . According to the relation (37), one expects $t_d \sim 1/L^2$. Inspection of Figure 9 shows that the data are consistent with the expected L -dependence for intermediate values of L .

For small L , there are strong deviations from this L -dependence for those τ -values which are closest to the transition temperature $\tau = \tau_u$. In fact, in the latter case, the decay time t_d increases with increasing L . This behavior represents a finite size effect since the size $L_{||}^*$ of the critical nucleus now satisfies $L_{||}^* \geq L$. In this case, one has to move the whole membrane segment over the potential barrier which corresponds to the activation free energy $\Delta\mathcal{F} \simeq \Delta V L^2$ (with $\Delta V = T\Delta U/a^2$) and thus to a decay time $t_d \sim \exp[\Delta V L^2/T]$ which grows with L .

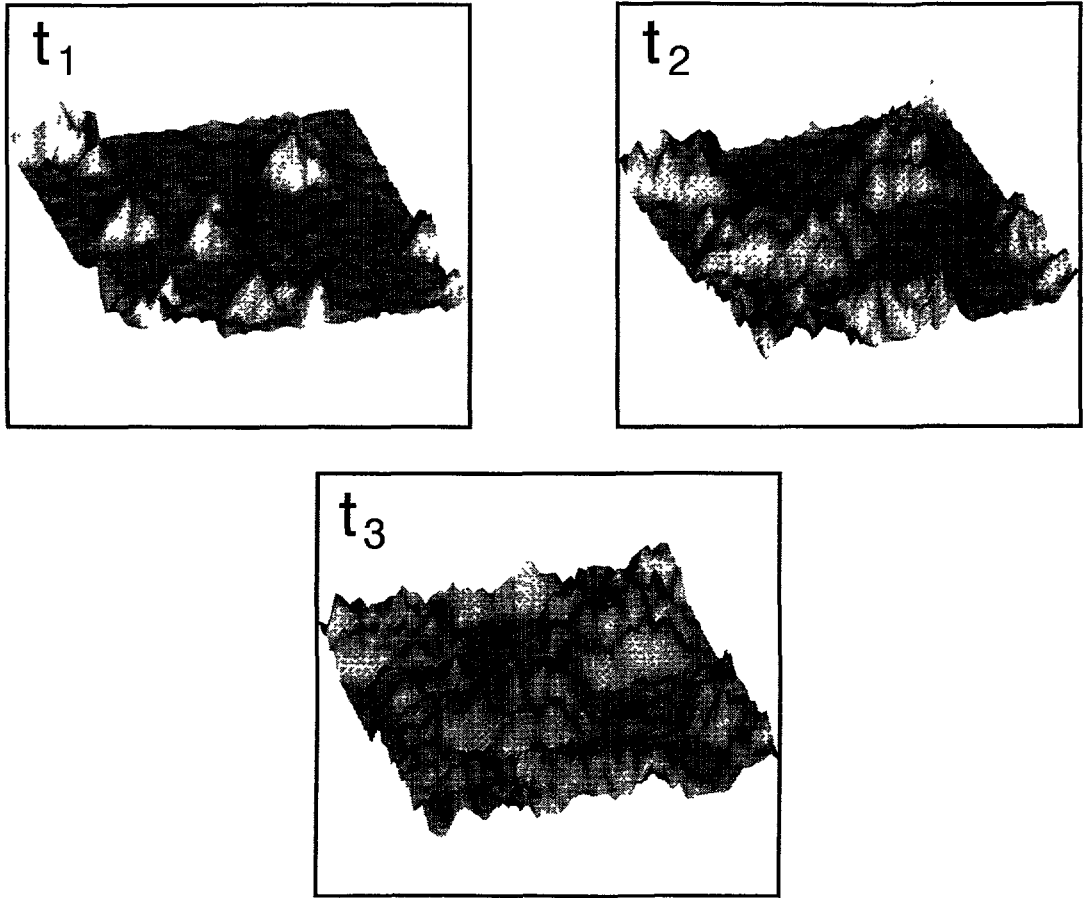


Fig. 10. — Growth of several islands for the temperature $\tau = -2.7$ and the linear sublattice size $n_s = 50$. The three snapshots are taken after $t_1 = 1.5 \times 10^3$, $t_2 = 2 \times 10^3$ and $t_3 = 2.5 \times 10^3$ MC steps.

On the other hand, for large L and for relatively large values of $\tau - \tau_u$, the decay time t_d decreases more slowly than $\sim 1/L^2$, see Figure 9. This is expected as soon as the metastable state decays via the nucleation of several critical islands, compare the estimate (39). One example for the time evolution of the membrane in such a situation is shown in Figure 10.

References

- [1] The Structure and Dynamics of Membranes, Vol. 1 of "Handbook of biological physics", R. Lipowsky and E. Sackmann Eds. (Elsevier, Amsterdam, 1995).
- [2] Verwey E. and Overbeek J., Theory of the stability of lyophobic colloids (Elsevier Publishing Company, Amsterdam, 1948).
- [3] Derjaguin B., Churaev N. and Muller V., Surface Forces (Consultants Bureau, New York, 1987).

- [4] Marra J. and Israelachvili J., *Biochem.* **24** (1985) 4608.
- [5] Lipowsky R., *J. Phys. II France* **4** (1994) 1755.
- [6] Lipowsky R., *Europhys. Lett.* **7** (1988) 255.
- [7] Canham P., *J. Theor. Biol.* **26** (1970) 61.
- [8] Helfrich W., *Z. Naturforsch.* **28c** (1973) 693.
- [9] Evans E., *Biophys. J.* **14** (1974) 923.
- [10] de Gennes P.-G. and Taupin C., *J. Phys. Chem.* **86** (1982) 2294.
- [11] Lipowsky R., in "Random fluctuations and Growth", G. Stanley and N. Ostrowsky Eds. (Kluwer Academic Publ., Dordrecht, 1988), pp. 227-246.
- [12] Amit D., *Field Theory, The Renormalization Group and Critical Phenomena* (McGraw-Hill, New York, 1978).
- [13] Milchev A., Herrmann D. and Binder K., *J. Stat. Phys.* **44** (1986) 749.
- [14] Grotehans S. and Lipowsky R., *Phys. Rev. A* **41** (1990) 4574.
- [15] Binder K., *Z. Phys. B* **43** (1981) 129.
- [16] Binder K. *et al.*, in "Dynamics of first order phase transitions", H. Herrmann, W. Janke and F. Karsch Eds. (World Scientific, Singapur, 1992) pp. 253-286.
- [17] Fisher M.E., in "Critical Phenomena", Proc. E. Fermi Int. School on Physics. M. Green Ed. (Academic, New York, 1971) p.1.
- [18] Barber M., in "Phase Transition and Critical Phenomena, C. Domb and M. Green Eds. (Academic Press, London, 1983) Vol. 8.
- [19] Abramowitz M. and Stegun I., *Handbook of mathematical functions*, tenth ed. (Dover Publications, New York, 1972).
- [20] Lee J. and Kosterlitz J., *Phys. Rev. B* **43** (1991) 3265.
- [21] McCoy B. and Wu T., *The two-dimensional Ising model* (Harvard University Press, Cambridge, Mass., 1973).
- [22] Lipowsky R. and Leibler S., *Phys. Rev. Lett.* **56** (1986) 2541.
- [23] Helfrich W., *Z. Naturforsch.* **33a** (1978) 305.
- [24] Lipowsky R. and Fisher M.E., *Phys. Rev. B* **36** (1987) 2126.
- [25] Becker R. and Döring W., *Ann. Phys.* **24** (1935) 719.
- [26] Abraham F., *Homogeneous Nucleation Theory* (Academic Press, New York, 1974).
- [27] Gunton J. and Droz D., *Introduction to the Theory of Metastable and Unstable States*, Vol. 183 of *Lecture Notes in Phys.* (Springer, Berlin, 1983).
- [28] Binder K. and Müller-Krumbhaar H., *Phys. Rev. B* **9** (1974) 2328.
- [29] D. Stauffer, in "Dynamics of first order phase transitions", H.J. Herrmann, W. Janke and F. Karsch Eds. (World Scientific, Singapore 1992) p. 287.